ELSEVIER

Journal of Power Sources 105 (2002) 66–74

JOURNAL OF POWER SOURCES

www.elsevier.com/locate/jpowsour

Study of the interface nickel/composite cathode of industrially made Li/V_2O_5 polymer (POE) batteries working at 90 °C

Pascal André[a], Philippe Deniard[a,*], Raymond Brec[a], Stéphane Lascaud[b]

[a]*Laboratoire de Chimie des Solides, I.M. Jean Rouxel, UMR 6502 CNRS 2, rue de la Houssinière, BP 32229, 44072 Nantes Cedex 03, France*
[b]*EDF, R&D Division, Electrical Equipment Department, CIMA Branch Site des Renardières, Route de Sens, Ecuelles, 77818 Moret sur Loing Cedex, France*

Received 14 April 2001; received in revised form 25 September 2001; accepted 1 October 2001

Abstract

$\omega Li/V_2O_5$ spirally wound polymer (POE) batteries functioning at 90 °C presented an important capacity fading ca. 20th cycle. This behavior could arise from the cathode material itself, including its in situ formation during the first reduction step from $\alpha Li/V_2O_5$, or from a technical problem linked either to the composite cathode or one of the other cell components. In this paper, after rejection of the two first hypothesis, we clearly demonstrate the negative role of the nickel foil used as cathodic collector.

Keywords: Lithium battery; V_2O_5; Polymer battery; Corrosion

1. Introduction

Experimental tests of industrially made batteries need all the components of the batteries in their industrial or pre-industrial setting. Within the frame of a collaboration with EDF, Bolloré and Institut des Matériaux Jean Rouxel (Contract 764971/EL777, no. OT M66L20), a complete electrochemical and structural study has been implemented on Li/V_2O_5 spirally wound polymer (POE) batteries functioning at 90 °C. During some preliminary studies of such industrially made generators, an important capacity loss appeared upon cycling around the 20th cycle (Fig. 1), a phenomenon not observed in laboratory liquid/polymer electrolyte cells.

This led to the analysis of the batteries different components, in particular, the composite cathode and the cathodic material α-V_2O_5 itself delivered by one of our industrial partners. It appeared [1] that its slight non stereochiometry (occurrence of extra $\{VO_2\}$ groups between the $\{VO_5\}$ pyramids of the α-V_2O_5 structure), was not sufficient to create a problem during the electrochemical intercalation of lithium as it was previously observed in $Fe_{0.12}V_2O_{5.15}$, a material presenting also extra cations in the V_2O_5 layers [2].

Other possible hypotheses for failure were tested since the origin of the dysfunction of these spirally wound batteries was not related to a structural feature of the pristine cathodic phase. In particular, it was thought that, since V_2O_5 undergoes several phase transitions upon lithium intercalation, the way to obtain the final NaCl-like structure (ω-$Li_3V_2O_5$) which is the phase on which the system then cycles, could be important. It was then decided to play upon the rate of the first discharge and also to study the battery interfaces. This last work was performed during the electrochemical functioning of the generators (chronopotentiometry at 90 °C) and during open circuit potential aging (impedance spectroscopy also at 90 °C). This study was followed by post-mortem EDXS analyses of both the positive electrode films and the interface positive electrode/nickel collector. XRD analyses of the intercalated positive material were also performed. The influence of the water remaining in the films following their fabrication has been demonstrated, and solutions to avoid the detrimental reaction of water are suggested.

2. Experimental

2.1. Preparation of the all solid state batteries

The Bolloré industrially made batteries are constituted by the stacking of a nickel foil (cathodic collector), a cathodic film (mainly α-V_2O_5 and poly-ethelene-oxide (PEO)), an electrolyte film (PEO + $LiCF_3SO_3$) and a lithium metal foil. The preparation method of the films and their assembly to constitute the spirally wound batteries have been described

* Corresponding author. Tel.: +33-2-40-37-39-38; fax: +33-2-40-37-39-95.
E-mail address: deniard@cnrs-imn.fr (P. Deniard).

0378-7753/02/$ – see front matter
PII: S0378-7753(01)00974-0

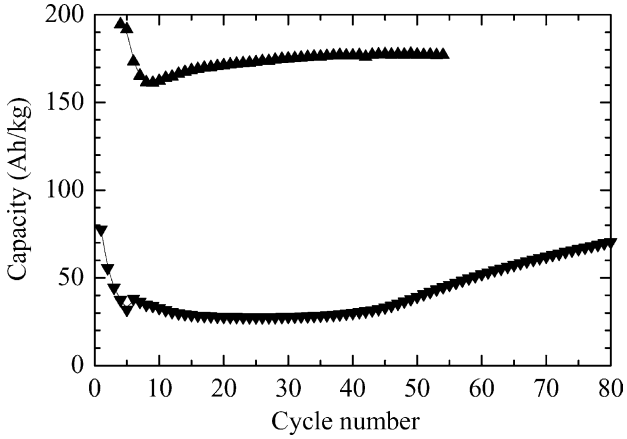

Fig. 1. Examples of capacity evolution on cycling of polymeric $Li_xV_2O_5$ cells at 90 °C in galvanostatic mode (*C*/20 in the 3.5–1.5 V interval). Capacity minimum ca. cycle #5 (▲) and drastic overall capacity loss ca. cycle #20 (▼).

elsewhere [1]. It is important to note (see Section 3.2.2) that some water remains in the electrolyte during the industrial process, in spite of drying of the film. This is the reason why some MgO with particle size of about 50 μm is added to eliminate water according to the reaction

$$MgO + H_2O \rightarrow Mg(OH)_2$$

The spirally wound generators under study were made from films 1 m long and 5 cm wide. Concerning the special tests cells, disks of 3 cm in diameter were cutout from the above films corresponding to a current of about 25 mAh for a first full discharge of three Li per V_2O_5. In order to protect the test cells from air, the flat disks were covered with resin. The post-mortem analyses were made after breaking of the resin coating by hammering and recovering of the battery disk.

2.2. X-ray diffraction

The cathodic films analyses of the cells were made with a D5000 Bruker diffractometer (Bragg–Brentano configuration) without monochromator (Cu $K\alpha_1 = 1.540598$ Å and Cu $K\alpha_2 = 1.544390$ Å). The electrochemical cells were post-mortem analyzed on the positive interface after tearing off the nickel collector and not on the electrolyte side since attempts to remove the electrolyte film proved impossible. The Rietveld method [3] (GSAS program [4]) was used to refine the ω-V_2O_5 structure obtained after the cells first discharge.

2.3. EDXS analyses

The EDXS analyses were performed, like the X-ray diffraction analyses, on the positive interface on the collector side. The EDXS analyses of the positive edge were performed after making a cryofracture of the positive film. This consisted in dipping the positive and the electrolyte films in liquid nitrogen for a few seconds in order to stiffen them: then, bending the films allowed their sudden breaking revealing a very neat fracture easy to analyze by the EDXS technique.

2.4. Galvanostatic cycling

After setting, the cell at the operating temperature of 90 °C, the cycling was performed at a 25 mA/g discharge regime (0.2 mA/cm^2) and at a 12.5 mA/g charge regime (0.1 mA/cm^2). This corresponded for the batteries working normally, to about *C*/8 and *C*/16 rates for the discharges and charges, respectively. After a complete charge or discharge, the batteries were allowed to relax until d*U*/d*t* (change of voltage with time) became smaller than 5 mV/h. All the experiments were performed with a MacPile testing system [5].

2.5. Impedance spectroscopy

Cells in their initial state, that is before the first discharge, were studied by impedance spectroscopy, in order to determine if the origin of the disfunctioning observed during cycling originated in the cycling itself or more simply in the aging of the materials at 90 °C. The analysis system was made of with a frequency analyzer (Solartron SI 1255) coupled to an electrochemical interface (EG&G273A). The polarizations were made with a galvanostat–potentiostat monitored by a MacIntosh.

The spectroscopic impedance measurements were made between 0.01 Hz and 100 kHz, i.e. over seven decades, at a rate of five measurements per decade. During these measurements, the batteries were maintained at 90 °C. Typically, the measurements were made over 1 month with a frequency higher at the beginning of the experiment: five measurements the first week and two the following weeks.

3. Results and discussions

3.1. Functioning batteries

The first discharge of the all solid batteries tested at 90 °C presented a succession of plateaus to be attributed to the different $Li_xV_2O_5$ phases occurring upon progressive lithium intercalation. The final phase formed is ω-$Li_3V_2O_5$, and it is this three-dimensional compound (NaCl structure) which is electrochemically active upon subsequent cycling at room temperature (liquid electrolyte electrochemical studies by Delmas et al. [6]). These authors proved also that, under a *C*/108 regime and in the 3.8–1.9 V range, a 375 mAh/g capacity could be obtained. At a higher regime (*C*/25), and between 3.2 and 1.8 V, the capacity dropped to 200 mAh/g.

In the case of the polymer systems under study, with regime of *C*/8 and *C*/20 between 3.5 and 1.5 V, we obtained results quite similar to those of Delmas et al. [6]. However,

Table 1
Capacity minimum of batteries after different first discharge rates

$\alpha \rightarrow \delta$	$\delta \rightarrow \gamma$	$\gamma \rightarrow \omega$	Capacity minimum (mAh/g)
F[a]	F	F	15
F	F	S[b]	158
F	S	S	138
S	F	F	84
S	S	F	68
S	S	S	77

[a] F, fast *C*/3.
[b] S, slow *C*/60.

and rather frequently, a capacity minimum, more or less pronounced, was recorded, sometimes accompanied by an irreversible drop of capacity (Fig. 1). Typically, the capacity dropped below 150 mAh/g, the resistance of the cell reaching high values of about 800 Ω cm^2, with an energy yield of 82%. In some cases, the capacity re-increased slowly going back to slightly higher values.

We have first tried to find out if the origin of this disfunctioning was linked to the first discharge of the positive material which is formed from the electrochemically active phase ω-$Li_3V_2O_5$.

3.1.1. Influence of the first discharge

Considering the three domains from α-$Li_xV_2O_5$ to δ-$Li_xV_2O_5$, from δ-$Li_xV_2O_5$ to γ-$Li_xV_2O_5$ and from γ-$Li_xV_2O_5$ to ω-$Li_xV_2O_5$, it was decided to carry out the discharge in each bi-phased domain either under a slow (S) (*C*/60) or a fast (F) (*C*/3) regime (Table 1). This was done in order to study the influence of transition speed upon the electrochemical characteristics of the final ω-$Li_xV_2O_5$ material. No link could be found between the imposed phase transformation speed and the cycling characteristics of the batteries (at least within the chosen regimes). In particular, in many of the cases studied, a rather strong capacity minimum was observed ($15\ \text{mAh/g} < Q_{\min} < 158\ \text{mAh/g}$) between the tenth and the 20th cycle (Table 1). The way the final phase is obtained from the pristine material, is thus, not at the origin of the observed malfunctioning. The origin of the problem was then searched in the choice of the potential limits imposed upon the system.

3.1.2. Influence of the potential limits

In order to avoid a decomposition of the polymer electrolyte in the all solid PEO batteries, the battery voltage is generally limited to the 3.5–1.5 voltage window. A still narrower domain (3.2–1.8 V) has been chosen in our experiments. Fig. 2 shows the capacity evolution with cycling at a *C*/20 regime with the above imposed voltage limitation by comparison with the classical limitation range (3.5–1.5 V). The great similarity of the two curves demonstrates that narrower potential limits do not allow to eliminate the capacity minimum.

To complete this study, we studied the battery electrochemical characteristics after 40 cycles (to reach a relatively

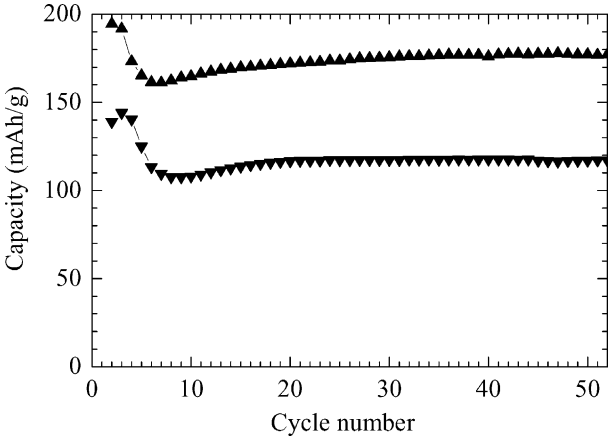

Fig. 2. Examples of capacity evolution on cycling of the polymeric $Li_xV_2O_5$ cells at 90 °C in galvanostatic mode (*C*/20): 3.5–1.5 V (▲); and 3.2–1.8 V (▼).

stable functioning) with different potential ranges (Fig. 3). Four successive potential windows were chosen within which 10 cycles were made: 3.5–1.5, 3.2–1.8, 3.5–1.8 and 3.2–1.5 V. It is to be observed that the choice of a 3.5 V upper potential instead of 3.2 V led to an over-potential quite high (300 mV instead of 90 mV) and that the choice of a lower potential (1.5 V instead of 1.8 V) induces the occurrence of a higher over-potential (400 mV instead of 200 mV). This implies that a widening of the potential window does not result in a capacity increase.

This last experiment confirmed that the capacity drop, at least, within the potential windows chosen, is not related to these windows. Post-mortem analyses of the batteries was then undertaken.

3.2. Post-mortem analyses of the spiraled wound batteries

Some, all solid state batteries were broken open after cycling 5, 20 and 35 times at a 25 mAh/g (*C*/8) discharge regime and at a 12 mAh/g (*C*/16) recharge regime. The different parts of the cells were then analyzed by scanning electron microscopy (SEM) and by EDXS.

3.2.1. Nickel collector analysis

The nickel collector shows on its surface grains of 1 μm long. Certain areas of these foils present parallel streaks due to the mill-processing. Before cycling, the nickel sheets presented, on their surface, an oxygen content of $2 \pm 1\%$, this concentration going up to $5 \pm 1\%$ after cycling. This analysis demonstrates that the collector has been oxidized upon the electrochemical cycling with the likely formation of an oxide, a hydroxide or an oxy-hydroxide (to be labeled NiO_xH_y in the following). The cause of the formation of NiO_xH_y is actually the presence of water in the polymer films of the cathode and electrolyte. Some of this water, absolutely necessary in the processing of the films made by extrusion by our industrial partner remains in the films in spite of a drying operation carried out afterwards. Indeed,

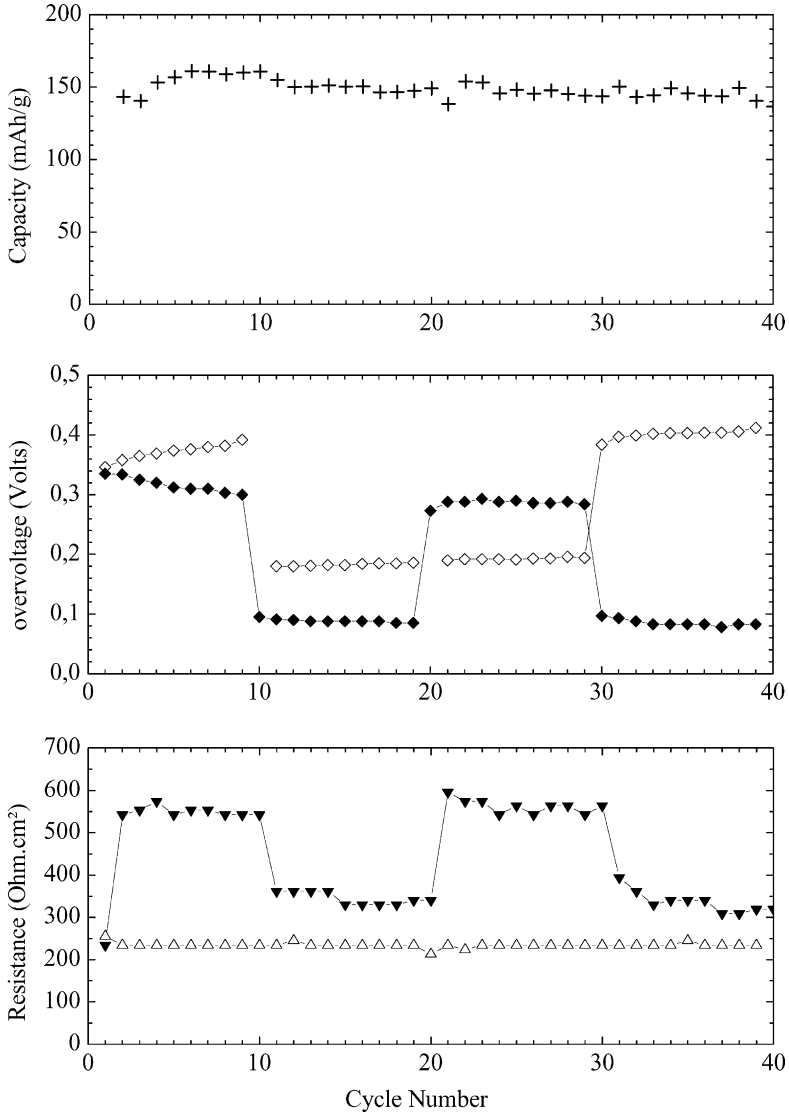

Fig. 3. Upper curves: cycling a polymeric $Li_xV_2O_5$ cells at 90 °C in galvanostatic mode (*C*/20). Cycles 1–10: 3.5 V < *U* < 1.5 V; cycles 11–20: 3.2 V < *U* < 1.8 V; cycles 21–30: 3.5 V < *U* < 1.8 V; and cycles 31–40: 3.2 V < *U* < 1.5 V. Middle curves: over-voltage after discharge (◆) and after charge (◇). Lower curve: resistance evolution of charged (▼) and discharged (△) cells.

no other components of the batteries can explain the oxidation of the collector considering the potential domain chosen.

Irrespective of the cycling duration, 10/20 μm micro-holes were systematically observed along the lamination direction. Around the micro-holes the oxygen concentration reaches 15% which is indicative of an important collector corrosion. Fig. 4 shows a typical micro-hole of about 20 μm in diameter. Such holes are at the center of clear disks with a diameter between 100 and 200 μm. The disks corresponding to zones in which the polymer may be strongly adhering to the collector surface. Retro-diffused electron images of the same area (Fig. 5) allowed us to see areas characterized by the occurrence of light elements. It can be due to the oxygen of V_2O_5 in places where the cathode remained glued to the nickel film, but around the micro-holes, it is to be attributed to a layer of NiO_xH_y.

3.2.2. Analysis of the composite cathode after 35 cycles

After 35 cycles, visual observations showed that the nickel collector is strongly oxidized. It was found important to check the possible effect that this oxidation might have on the cathodic films themselves. A series of EDXS analyses of the cathode surface at the interface with the nickel collector was then carried out. These analyses showed a rather important amount of nickel (between 2.5 and 10% depending on the areas, with an average around 6%). This led us to check the occurrence of nickel within the composite cathode itself, to see if a possible diffusion of the oxidized species had happened.

Fig. 6 gives the cross section of a cathode with the various spots where the analyses were performed and the various elemental percentages of the elements found in the cathode and the electrolyte. The LiTFSI concentrations were determined by an analysis of sulfur since it is present not only in the cathode (7% w/w), but also in the electrolyte (18% w/w).

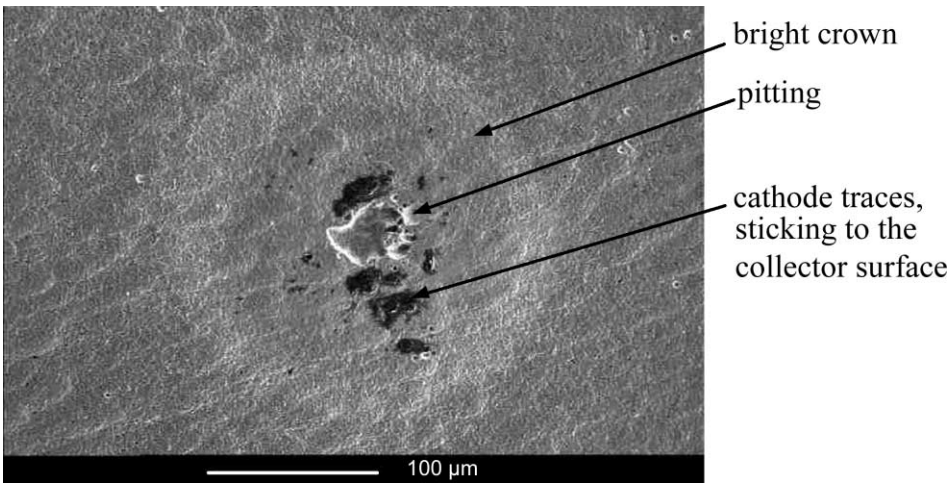

Fig. 4. SEM image of a nickel foil used as cathodic collector in a polymeric $Li_xV_2O_5$ cell after 35 cycles at 90 °C.

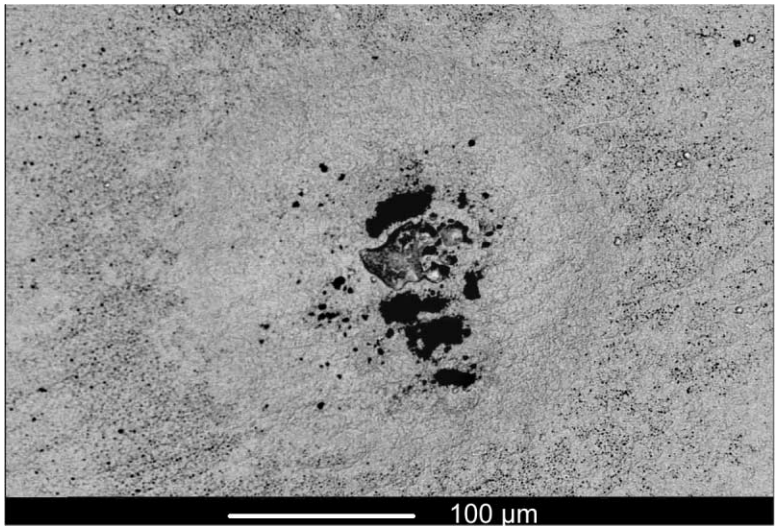

Fig. 5. SEM image (back scattered electrons) of a nickel foil used as a cathodic current collector in a polymeric $Li_xV_2O_5$ cell after 35 cycles at 90 °C. Dark zones correspond to elements with low atomic number (cathode traces, nickel oxide or hydroxide).

The other element analyses have been standardized against these two known values. Let us mention that the vanadium and magnesium concentrations allowed us to discriminate the frontier between the cathode that contains vanadium, but no magnesium and the electrolyte containing magnesium, but no vanadium. It is to be mentioned that MgO is added to the electrolyte [1] in order to partially trap the water added during the film processing.

The analyses showed that an important amount of nickel has diffused inside the cathode (about 60 mg/cm^3 in average). Clearly, nickel has penetrated inside the cathodic material, crossing the collector/cathode/interface. Notice that the nickel content decreases as the analyses are made further away from the collector.

3.2.3. Analysis of the cells after between 5 and 35 cycles

In order to follow the occurrence of this diffusion phenomenon, other batteries were cycled over different times and then analyzed for the above elements. The results (Table 2) indicate that in a first step, the oxygen concentration increases at the collector surface (up to 8(1)%) then decreases upon cycling. This result can be interpreted as corresponding first to the formation of an NiO_xH_y passivation layer at the collector/cathode interface then to its migration into the cathodic film.

This analysis of the collector after cycling shows clearly that the capacity minimum, located around the 20th cycle, is

Table 2
EDXS analyses results at the cathode//electrolyte interface and in the cathode bulk for different cycling modes

Last cycle	Oxygen on the collector (wt.%)	Nickel on the cathode (wt.%)	Nickel into the cathode (wt.%)
5	5 (1)	0	0
20	8 (1)	0	0
35	6 (1)	6 (1)	2 (1)

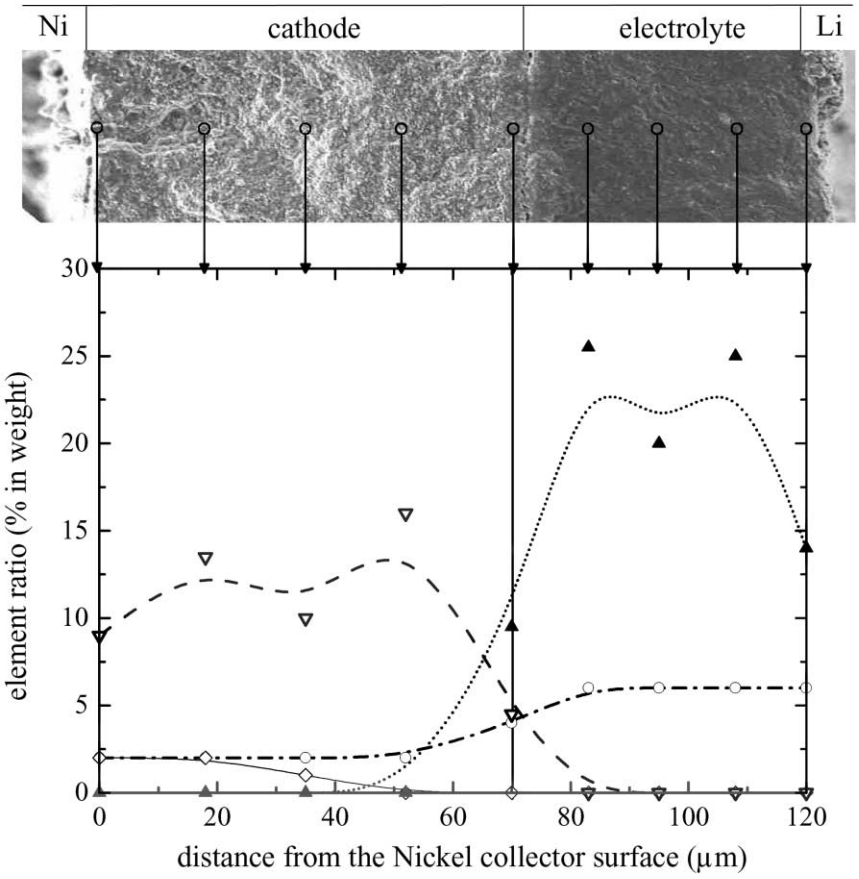

Fig. 6. SEM image of the electrolyte and the cathode (after a cryofracture) of a polymeric $Li_xV_2O_5$ cell after 35 cycles (upper part) and concentration of some elements of the cathode and of the electrolyte (EDXS analyses): S (○) for LiTFSi; Ni (◇) for nickel oxide and/or hydroxide; V (▽) for α-V_2O_5; and Mg (▲) for MgO. Nickel does appear in the cathode bulk, but does not seem to have diffused through the cathode/electrolyte interface.

to be linked to a passivation phenomenon of the collector/cathode interface. In effect, the formation of a passivation layer increases the interfacial impedance, inducing a strong decrease of the capacity due to the potential window shift as observed during the functioning of the batteries. The passivation layers then tends to disappear, NiO_xH_y diffusing into the cathodic film and leading to an increase of the capacity over about a score of cycles.

The passivation reaction can only be attributed to the occurrence of water inside the polymer films since no other part or compound of the cell can be oxidized. This also raises incidentally the role of cycling on this phenomenon, since the passivation/dissolution mechanism observed may be related either to time (aging) or to cycling or both. To study the aging influence, a series of all solid state batteries have been studied prior to any discharge and analyzed by impedance spectroscopy.

3.3. Impedance spectroscopy analysis on spirally wound batteries prior to cycling

Observing some cycled battery impedance spectra, three arcs are observed (Fig. 7) corresponding to weak capacities (from 0.1 to 1 μF), medium capacities (around 10 μF) and high capacities (about 104 mF). The arcs with weak and medium capacities also appear in the spectra of the half cells Ni//cathode, showing that they are characteristic of the interface between the nickel collector and the cathode film. Fig. 8 shows the imaginary and real part of the impedance versus frequency of a typical cell during aging at 90 °C prior to cycling. Important changes of the electronic characteristics are recorded during the first month with, in particular, the arc corresponding to the medium capacity seeing its associated resistance increase from 20 to 300 Ω in 5 days. After 20 days, it decreases to 30 Ω, then remains quasi-constant (Fig. 9). The type of representation in Fig. 8 has been preferred to the representation of the impedance spectra versus frequency because the dispersion of the impedance data did not allow to compare easily the various spectra. The changes in the characteristics of this arc shows clearly that the interface nickel/cathode is the object of a transitory phenomenon. It appears, thus, that the passivation reaction observed by EDXS analyses is not due to the cycling (at least not entirely), but rather to the oxidation reaction at 90 °C at the cells interface, the capacity minimum corresponding in fact, after about 1 week, to a

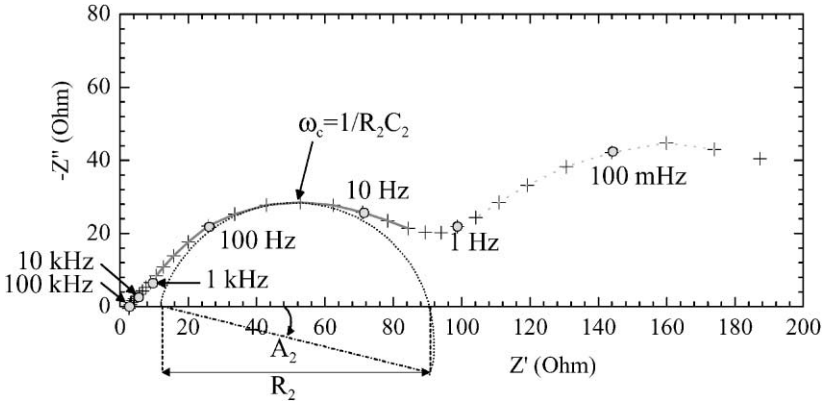

Fig. 7. Impedance spectra of a polymeric $Li_xV_2O_5$ cell at 90 °C: A_2 is the shift angle toward the abscissa axis; R_2 is the corresponding resistance; ω_2 is the characteristic frequency of the circle; and C_2 corresponds to its capacity.

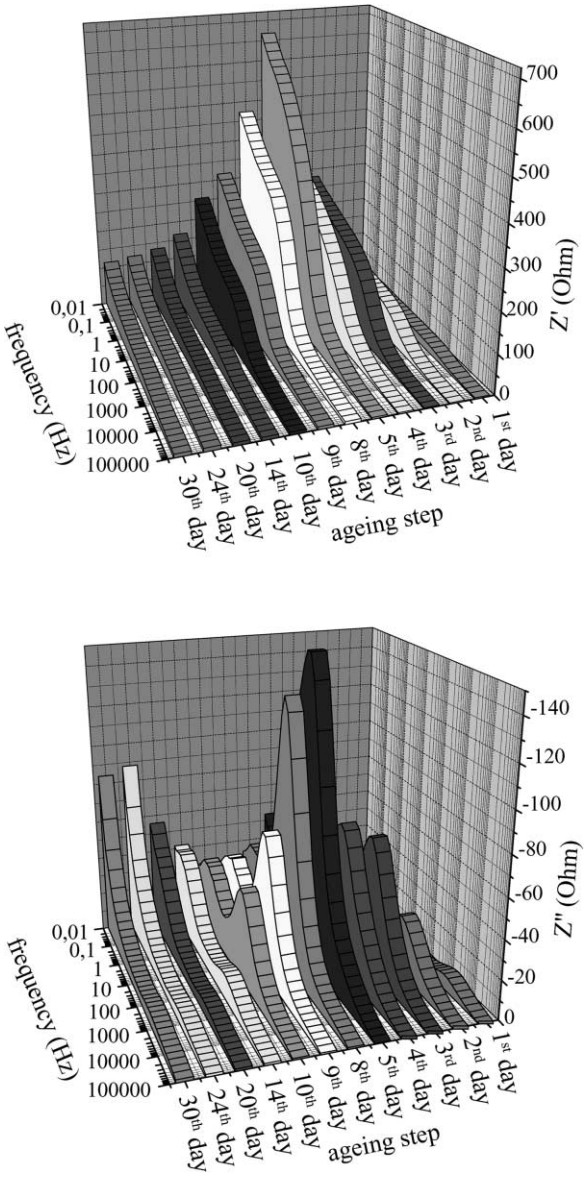

Fig. 8. Impedance evolution of a polymeric $Li_xV_2O_5$ cell aged at 90 °C prior to cycling. Upper curve, real part; lower curve, imaginary part. The maximum is reached at the end of the first week.

maximum in the transfer resistance. In a first step, this analysis confirms the formation of a passivating layer at the nickel/cathode interface, the insulating layer increasing the transfer resistance, followed by a dissolution of this passivating layer inducing a decrease of the transfer resistance. This explains well that upon cycling, the capacity first drops then increases. This hypothesis has been confirmed by the experiment consisting either in aging the batteries before their cycling (allowing for a complete dissolution of the passivating layer) or in using an non-oxidizable collector (avoiding the formation of any passivating coating on the collector).

3.4. Aging prior to cycling

A spirally wound battery was aged 30 days at 90 °C, then cycled at a *C*/20 rate in an galvanostatic mode (Fig. 10). It is observed that the first discharge curve is slightly different from that of a non-aged battery because of some self-discharge during aging. Then a very good cycling is recorded, with an initial capacity of 240 mAh/g, with a small decrease beyond the 25 first cycles (225 mAh/g at the 25th cycle). The cycling characteristics are stable, with in particular a constant resistance of 100 Ω cm^2, whereas a value of about 800 Ω cm^2 was observed for the non-aged batteries. On the other hand, the faradic yield is 100%, which indicates an absence of current leak, and the energetic yield is also higher than in the cases of the non-aged generators, 86/87% instead of 80/82%. This experiment demonstrates that it is possible to overcome the detrimental effect of the nickel oxidation in our $Li_xV_2O_5$/PEO industrial batteries by annealing them during several weeks at 90 °C. The explanation of such a phenomenon lies in a fast oxidation of the nickel foil by the residual water, forming a NiO_xH_y passivating layer. During the aging at 90 °C, the NiO_xH_y species diffuses rapidly into the cathode. Hence, the passivating layer width decreases, leading to a proper functioning of the battery. Beyond this aging, another possibility is the use of a non-reactive current collector, and this has been tested as explained in Section 3.5.

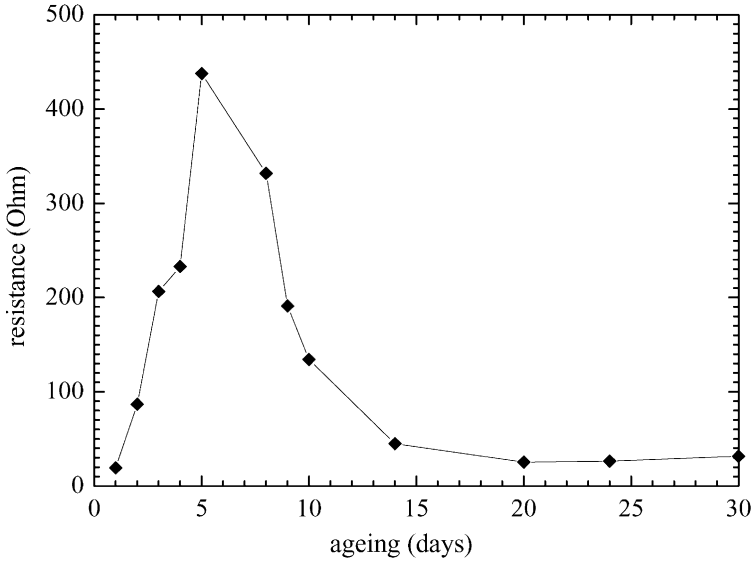

Fig. 9. Resistance evolution of a polymeric $Li_xV_2O_5$ cell aged at 90 °C corresponding to the 10 μF circle.

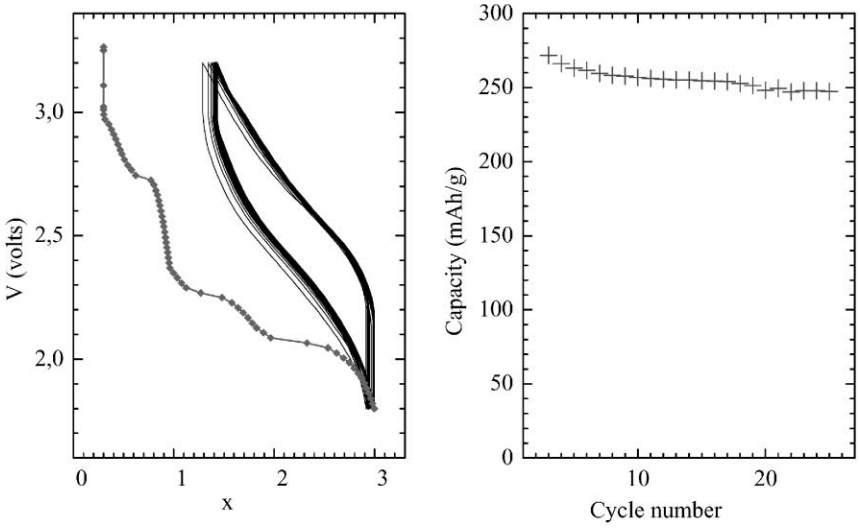

Fig. 10. Cycling characteristics (*C*/20 in galvanostatic mode) of a polymeric $Li_xV_2O_5$ cell aged at 90 °C during 30 days. Left, cycling curve; right, capacity evolution.

3.5. Cycling of a PEO battery with a non-oxidizable collector

The study of the influence of water on battery cycling has been carried out with the use of gold as the positive current collector, since this element will not be oxidized in the system. The battery was hand made, the spirally wound generators being fabricated from extrusion only from important quantities of the elements (no less that 1 kg of α-V_2O_5 for instance) and large surface collector sheets. The results obtained in this case are much better that those obtained with the nickel foil (Fig. 11), with in particular weaker resistances (less than 200 Ω cm). The energy yield remains elevated (above 85% versus 80/82% in the classical batteries) and the faradic yield does not drop until the 18th cycle. However, the use of a gold collector did not prevent the occurrence of some leakage, whose origin could not be determined. These global improvements of the cycling characteristics go along with a very good value of the discharge capacity. On the 10th cycle, the capacity is 50% above that of the reference battery mentioned before, that is to say 230 mAh/g (to be compared to 150 mAh/g). It remains high after 25 cycles (216 mAh/g) and is quite satisfactory beyond 80 cycles (190 mAh/g). It is to be noted, however, that the faradic yield is weak (dropping to 50% at the 59th cycle), in relation with the important current leak mentioned above. Nevertheless, this experiment does not invalidate our conclusions that on the batteries with a nickel collector, the dysfunction is due to collector oxidation.

Another set of experiments was performed with a nickel collector coated with gold. The coat was deposited by

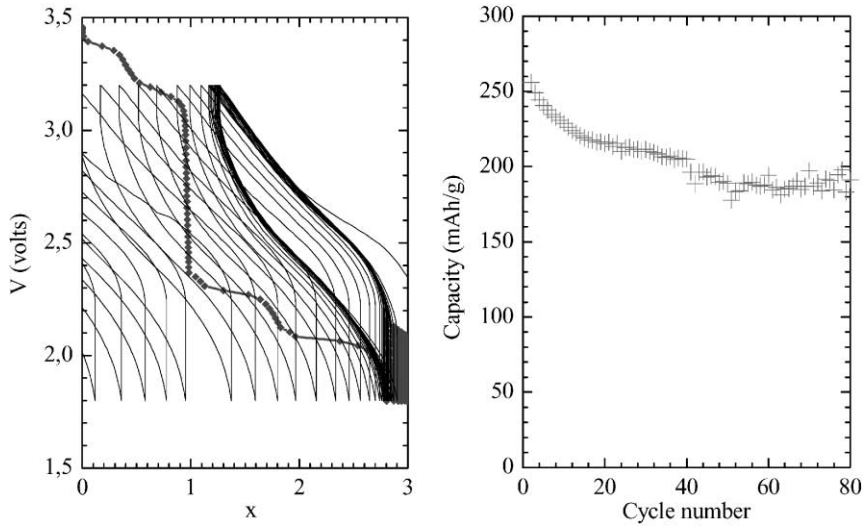

Fig. 11. Cycling characteristics of a polymeric $Li_xV_2O_5$ cell at 90 °C (*C*/20 in galvanostatic mode) with a gold collector. Left, cycling curve; right, capacity evolution.

cathodic sputtering and was about 100 Å thick. The experiments carried out in the same electrochemical cycling conditions as above yielded the same type of results as with the solid gold collector. This fundamental study was carried out to demonstrate the nickel collector oxidation, hence, the use of gold. For practical purpose, other metal collectors are currently being tested.

3.6. Conclusion

The study performed on the $Li_xV_2O_5$/POE, LiTSFI/Li batteries has shown that the increase of the resistance of the generators and the capacity loss are to be related to the presence of water in the batteries. In a first step, the water oxidizes the nickel collector surface with the ensuing formation of a passivating layer. This explains the increase of charge transfer resistance at the nickel/cathode interface. In a second step, the passivating layer (probably made of nickel oxide or oxy-hydroxide $Ni_xO_yH_z$) diffuses into the cathodic material. This diffusion of the passivating layer explains the resistance drop of the electrode. This phenomenon takes place in the batteries upon cycling, but cycling itself does not seem to have much influence on the formation of the passivation layer. In effect, a 30-day aging of the batteries maintained at 90 °C shows very good values and stability of the electrochemical properties once the passivating layer has diffused into the cathode film. Among the solutions that can be envisioned to solve this problem (water presence being necessary in the PEO films extrusion process), we suggest either a storing of the spirally wound batteries once fabricated at 90 °C for 3–4 weeks or the changing of the nickel positive collector by another metal. An alternative solution would consist in modifying the battery process banning any water use, but this does not seem practical.

References

[1] P. André, P. Deniard, R. Brec, Solid State Sci., 2001, in press.
[2] S. Maingot, P. Deniard, N. Baffier, J.-P. Pereira-Ramos, A. Kahn-Harari, R. Brec, Mater. Sci. Forum 152/153 (1994) 297.
[3] H.M. Rietveld, J. Appl. Crystallogr. 2 (1962) 65.
[4] A.C. Larson, R.B. von Dreele, Generalized structure analysis system (GSAS), Los Alamos National Laboratory Report no. LA-UR-86-748.
[5] C. Mouget, Y. Chabre, MacPile, Licensed from CNRS and UJP Grenoble to Bio-Logic, 1, Av. de l'Europe, 38640 Claix, France.
[6] C. Delmas, S. Brethes, M. Ménetrier, Solid State Ionics 34 (1991) 113.